Molecular Dynamics Investigations of Thermomechanical Characteristics of Solid and Hollow Spherical Platinum Nanoparticles during Additive Manufacturing

Ling-Feng Lai,[1] Deng-Maw Lu,[1] Jian-Ming Lu,[2]* Yu-Chen Su,[3] and Kuei-Shu Hsu[4]**

[1]Department of Mechanical Engineering, Southern Taiwan University of Science and Technology,
Number 1, Nantai Street, Yungkang District, Tainan City 710301, Taiwan
[2]National Center for High-Performance Computing, National Applied Research Laboratories,
Number 28, Nan-ke 3rd Road, Hsin-Shi District, Tainan City 744094, Taiwan
[3]Department of Civil Engineering, National Central University,
Number 300, Zhongda Road, Zhongli District, Taoyuan City 320317, Taiwan
[4]Department of Applied Geoinformatics, Chia Nan University of Pharmacy & Science
Number 60, Sec. 1, Erren Road, Rende District, Tainan City 717301, Taiwan

The molecular dynamics simulation method with the embedded atom model/Finnis–Sinclair potential was used to investigate solid and hollow spherical platinum (Pt) nanoparticles under different heating rates during the additive manufacturing process. We concluded that the coalescence temperatures of solid and hollow spherical Pt nanoparticles range between 975 and 1450 K and between 561 and 1414 K, respectively. We concluded also that the melting temperatures of solid and hollow spherical Pt nanoparticles range between 1300 and 1535 K and between 1250 and 1500 K, respectively. In this study, we found that the lower the heating rate, the greater the diffusion of Pt atoms. The solid-state sintering of Pt nanoparticles can spontaneously occur at 300 K. We concluded that the melting temperatures of both solid and hollow spherical Pt nanoparticles are still lower than the macroscopic melting point of Pt (2041.4 K).

1. Introduction

The additive manufacturing (AM)[1–4] technology is divided into seven categories, among which there are two technologies applied to metallic powder: powder bed fusion (PBF)[5] and laser metal deposition (LMD). The substances manufactured by the PBF technology are rougher and more precise than those made by other mechanical manufacturing processes, such as precision casting, turning, and forging, and complex and integrally formed structures can be produced. PBF can produce metallic supports without modular jigs and fixtures, whereas LMD can produce, coat, and repair curved metallic surfaces. Pt is a precious metal with high density,

ductility, corrosion resistance, and low reactivity. Pt can be used in electrodes, resistors, turbine engines, dental filling materials, anticancer drugs, and accessories. In addition, glass coated with a Pt film has an opaque side and a transparent side, enabling one-way light transmission.

In this study, molecular dynamics (MD)[6] is used to simulate solid and hollow spherical Pt nanoparticles under different parameter conditions by AM. The coalescence temperature, melting temperature, and crystalline structure[7–9] were determined.

2. Materials and Methods

2.1 MD simulations

MD was derived from classical Newtonian mechanics.[10] MD with suitable potential functions can simulate, for example, atomic positions, trajectory, and forces. The large-scale atomic/molecular massively parallel simulator (LAMMPS)[11] based on MD is an open source program written and compiled in C++. LAMMPS can simulate the internal structure, thermodynamics, dynamics, and force of metallic nanoparticles. In this study, LAMMPS is used to simulate the thermomechanical properties, including the coalescence and melting temperatures of nanoscale Pt during AM.

2.2 Atomic model preparation

2.2.1 Solid nanoparticles

In this study, solid and hollow spherical Pt nanoparticles are simulated by LAMMPS, nonperiodic boundary conditions are set for the parameters, the canonical ensemble is given, and the initial structure of Pt is the face-centered cubic (FCC) crystal structure. The disordered atomic structure is set on the outer surface of Pt nanoparticles, and the space of the simulation box is several times larger than that of solid and hollow spherical Pt nanoparticles. The initial gap between the Pt nanoparticles is set to 5 Å, the lattice constant is set to 3.9201 Å, and the sizes of the Pt nanoparticles are 16a, 20a, and 24a. There are three groups of identical nanoparticle sizes and three groups of different nanoparticle sizes, as shown in Table 1 and Fig. 1.

2.2.2 Hollow nanoparticles

A hollow spherical Pt nanoparticle is formed by removing the inner atoms of a solid spherical Pt nanoparticle by LAMMPS, as shown in Table 1 and Fig. 1.

2.3 Auxiliary analysis and calculation

LAMMPS with EAM/FS potential[12] can describe the force of interactions[13] between Pt atoms, and the positions and trajectories of each Pt atom of solid and hollow spherical Pt nanoparticles at each time step during AM, where the electron density is obtained from the wave

Table 1
Parameters and number of atoms of the Pt nanoparticle model. (a) Solid and (b) hollow.

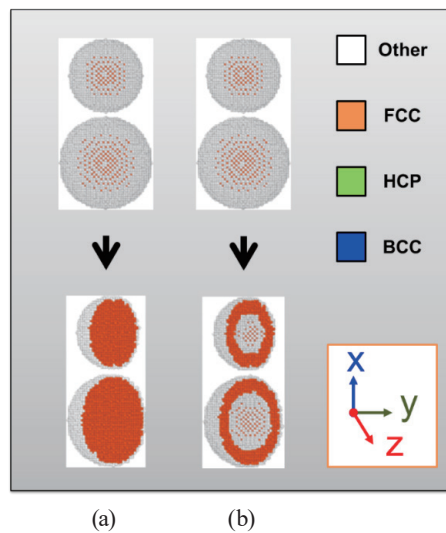| Type (D1–D2)	Structure	Atoms
16a–16a		17178
16a–20a		25346
16a–24a	Solid	37486
20a–20a		33514
20a–24a		45654
24a–24a		57794
16a–16a		15056
16a–20a		20696
16a–24a	Hollow	27836
20a–20a		26336
20a–24a		33476
24a–24a		40616

Fig. 1.   (Color online) Cross-sectional view of Pt nanoparticles: (a) solid and (b) hollow models.

function, and then the atoms that must be calculated for each atomic energy are embedded in the local electron density energy.[14] The fitting method has been proposed by Daw *et al.*[15]

The common neighbor analysis[16] can simulate both solid and hollow spherical Pt nanoparticles in AM and visualize each lattice structure at each time step. The gyration radius (Rg) is used to calculate the mean square displacement (MSD)[17] between atoms and the center of mass of both solid and hollow spherical Pt nanoparticles in AM. In Eq. (1) below, the total mass of the space is M, the center of mass is r_{cm}, the position of each atom in the nanoparticle is r, and the subscript i indicates the type of atom in the space.[18]

$$R_g^2 = \frac{1}{M}\sum_i m_i \left(r_i - r_{cm}\right)^2 \tag{1}$$

MSD is an important parameter and it is the average distance between Pt atoms. The total mass of the space is N, the position of each atom in the nanoparticle is r, the time is t, and the subscript i indicates the type of atom in the simulated environment space.[19]

$$MSD = \frac{1}{N}\sum_i \left[r_i(t) - r_i(0) \right]^2 \qquad (2)$$

3.   Results and Analysis

3.1   Solid nanoparticles

3.1.1   Thermal equilibration at room temperature

In this study, LAMMPS is used to simulate solid and hollow spherical Pt nanoparticles, and the internal lattice structure, force, and trajectory of the Pt nanoparticles are observed at a room temperature of 300 K. The four points, Points A, B, C, and D, correspond to the four states shown in Fig. 2. In Fig. 2, Point A indicates solid spherical Pt nanoparticles to maintain the initial gap of 5 Å, the Rg of solid spherical Pt nanoparticles is 45.22 Å, the neck width is 0 Å, FCC accounts for 80.24%, hexagonal close packing (HCP) accounts for 0%, and the others account for 19.76% of state A. As shown in Fig. 2, the small size effect at Point B of solid spherical Pt nanoparticles causes the solid spherical Pt nanoparticles to coalesce together. At Point B, Rg is 45.21 Å, the neck width is 31.55 Å, FCC accounts for 80.46%, HCP accounts for 0%, and the others account for 19.54% of state B. At Point C in Fig. 2, the Rg of solid spherical Pt nanoparticles is 45.21 Å, the neck width is 40.56 Å, FCC accounts for 78.21%, HCP accounts for 0.39%, and the others account for 21.40% of state C. At Point D in Fig. 2, the Rg of solid spherical Pt nanoparticles is 44.13 Å, the neck width is 40.05Å, FCC accounts for 80.87%, HCP accounts for 0.08%, and the others account for 19.05% of state D.

3.1.2. Laser sintering

In this study, LAMMPS was used to simulate the solid spherical Pt nanoparticles during AM. As shown in Fig. 3, the solid spherical Pt nanoparticles heated at 0.25 K/ps are divided into four
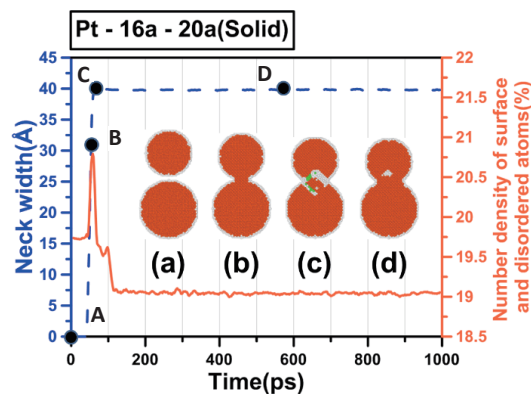

Fig. 2.   (Color online) Solid spherical Pt nanoparticles for the combination 16a-20a in Table 1 are shown. At room temperature, the neck width changes with the density of surface disordered Pt atoms with different time steps.
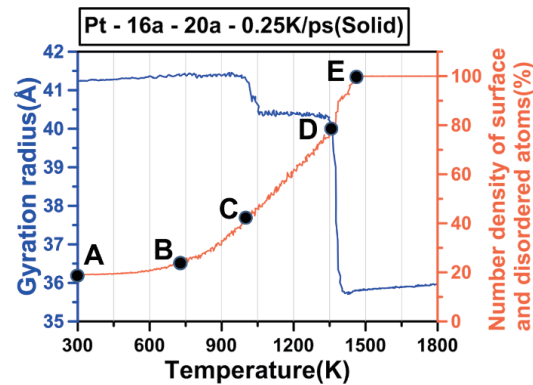
Fig. 3.   (Color online) Solid spherical Pt nanoparticles of 16a-20a were sintered using a laser at 0.25 K/ps in the range of 300–1800 K. The changes in Rg and density of surface disordered Pt atoms are plotted.

sections by five points, Points A, B, C, D, and E. From Points A to C, solid spherical Pt nanoparticles are relatively stable. The area between Points C and D in Fig. 3 is the region of atomic coalescence. After being heated using a laser, the nanoparticles coalesce together. In Fig. 3, from Points D to E, solid spherical Pt nanoparticles gradually melt, and the internal lattice structure changes considerably. Beyond Point E in Fig. 3, the Pt nanoparticles are completely melted.

Figure 4 shows the change in the MSD of the solid spherical Pt nanoparticles heated linearly at heating rates of 1, 0.5, and 0.25 K/ps during AM. It is found that the diffusion effect of the Pt nanoparticles is best at 0.25 K/ps since the MSD of Pt is the largest.

Figures 5 and 6 respectively show that the coalescence temperature is between 975 and 1450 K and that the melting temperature is between 1300 and 1535 K for solid spherical Pt nanoparticles during AM.[19]

3.2   Hollow nanoparticles

3.2.1   Thermal equilibration

In this study, LAMMPS is used to simulate hollow spherical Pt nanoparticles, and the internal lattice structures, forces, and trajectories of Pt are observed at a room temperature of 300 K. Four states, (a), (b), (c), and (d), are shown in Fig. 7. In Fig. 7, Point A indicates hollow spherical Pt nanoparticles to maintain the initial gap of 5 Å, the *Rg* of the hollow spherical Pt nanoparticles is 46.70 Å, the neck width is 0 Å, FCC accounts for 66.88%, HCP accounts for 0%, and the others account for 33.12%. As shown in Fig. 7, the small size effect at Point B of the hollow spherical Pt nanoparticles causes the hollow spherical Pt nanoparticles to coalesce together. At Point B, *Rg* is 46.70 Å, the neck width is 29.72 Å, FCC accounts for 66.73%, HCP accounts for 0%, and the others account for 33.27% of state B. At Point C in Fig. 7, the *Rg* of hollow spherical Pt nanoparticles is 46.70 Å, the neck width is 31.34 Å, FCC accounts for 66.31%, HCP accounts for 0.06%, and the others account for 33.63% of state C. At Point D in Fig. 7, the *Rg* of hollow spherical Pt nanoparticles is 46.69 Å, the neck width is 35.53 Å, FCC accounts for 67.55%, HCP accounts for 0%, and the others account for 32.45% of state D.
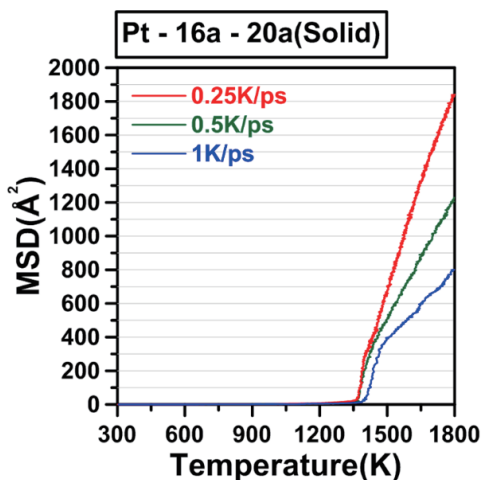
Fig. 4.   (Color online) Temperature change vs MSD of solid spherical Pt nanoparticles of type 16a-20a solid model at heating rates of 0.25, 0.5, and 1 K/ps in the range of 300–1800 K.
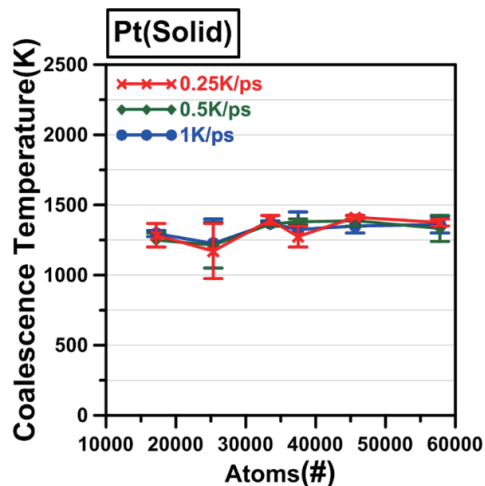

Fig. 5.   (Color online) Coalescence temperature as a function of number of atoms between 10000 and 60000 for solid spherical Pt nanoparticles with three heating rates.
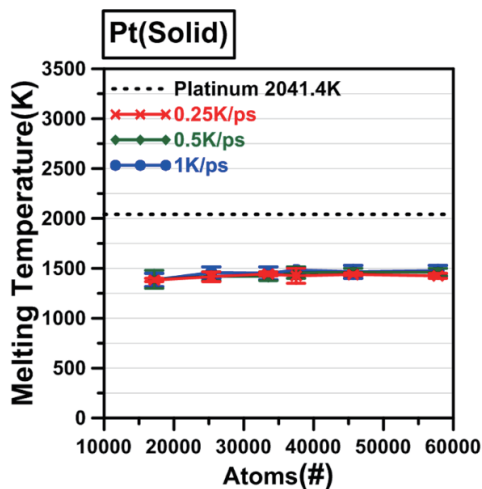

Fig. 6.   (Color online) Melting temperature as a function of number of atoms between 10000 and 60000 for nanoscale solid spherical Pt nanoparticles with three heating rates. The dashed line shows the macroscopic melting point of Pt (2041.4 K).
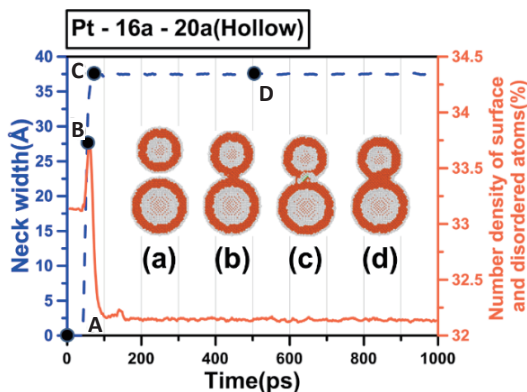

Fig. 7.   (Color online) Hollow spherical Pt nanoparticles are illustrated as the combination of 16a–20a. The neck width and the density of surface disordered Pt atoms at room temperature are shown at different points in time.

3.2.2   Laser sintering

As shown in the results of the laser sintering process in Fig. 8, hollow spherical Pt nanoparticles heated at 0.25 K/ps are divided into four sections by five points, Points A, B, C, D, and E. From Points A to C, the nanoparticles are relatively stable. The coalescence stage is from Points C to D. The melting stage is from Points D to E. Beyond point E, the Pt nanoparticles are completely melted.

From the results shown in Fig. 9, it is concluded that the MSD of hollow spherical Pt nanoparticles heated at 0.25 K/ps is larger than those heated at 1 and 0.5 K/ps. In other words, the diffusion of Pt atoms is more rapid and slower at higher and lower heating rates, respectively. The higher the heating rate, the slower the Pt atom diffusion, and vice versa.

Figures 10 and 11 show that for hollow spherical Pt nanoparticles heated using a laser, the coalescence temperature is in the range of 561–1414 K and the melting temperature is between 1250 and 1500 K, respectively.[19]
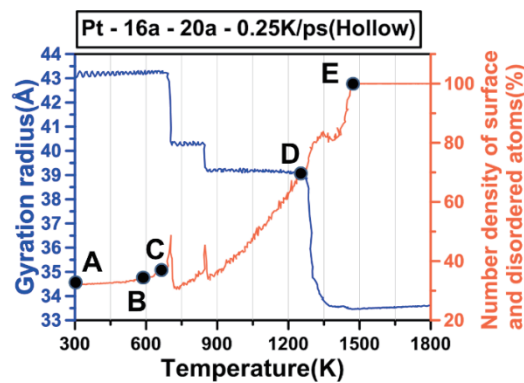

Fig. 8.   (Color online) Hollow spherical Pt nanoparticles of 16a-20a were sintered using a laser at 0.25 K/ps in the range of 300–1800 K. The change in Rg and the density curve of surface disordered Pt atoms are plotted.
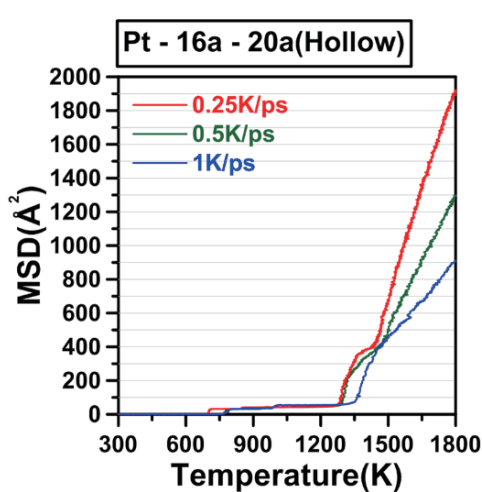

Fig. 9.   (Color online) MSD vs temperature for hollow spherical Pt nanoparticles of 16a–20a heated at rates of 0.25, 0.5, and 1 K/ps between 300 and 1800 K.
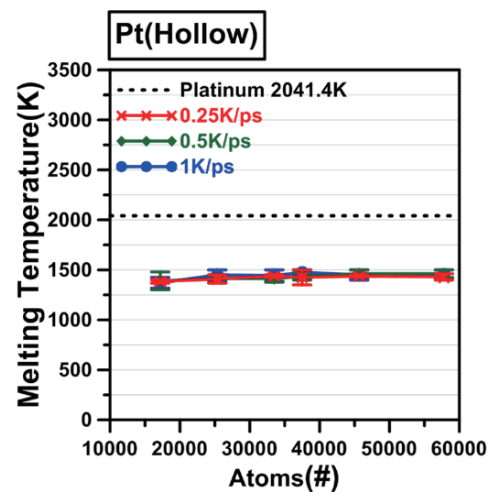
Fig. 10.   (Color online) Coalescence temperature as a function of number of atoms between 10000 and 50000 for hollow spherical Pt nanoparticles at three heating rates.
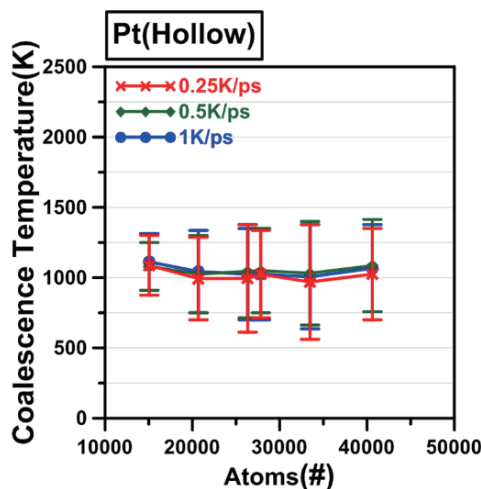
Fig. 11. (Color online) Melting temperature as a function of number of atoms between 10000 and 60000 for nanoscale hollow spherical Pt particles at three heating rates. The dashed line shows the macroscopic melting point of Pt (2041.4 K).

4. Conclusions

The LAMMPA results of MD simulations were used for the comparative study of Pt nanoparticles with different sizes during AM. Three heating rates of 0.25, 0.5, and 1 K/ps were considered. The findings of this study are as follows.

(1) Solid-state sintering can occur for the simulated Pt nanoparticles at a room temperature of 300 K. During the sintering of Pt nanoparticles, crystal defects temporarily appear in the simulated Pt nanoparticles. The above phenomenon of Pt nanoparticles is caused by the high ratio of surface area to volume.

(2) Hollow spherical Pt nanoparticles have more surface Pt atoms than solid Pt nanoparticles because of a higher ratio of surface area to volume.

(3) The higher the heating rate, the slower the diffusion of Pt atoms, and vice versa.

(4) The coalescence temperatures of solid and hollow spherical Pt nanoparticles were between 975 and 1450 K and between 561 and 1414 K, respectively. Their melting temperatures were between 1300 and 1535 K and between 1250 and 1500 K, respectively. The melting temperatures of both solid and hollow spherical Pt nanoparticles are still lower than the macroscopic melting point of Pt (2041.4 K).[19]

(5) The melting temperature of nanoscale solid and hollow spherical Pt nanoparticles is much lower than the melting point of Pt (2041.4 K).

Acknowledgments

We are thankful for the computation time, resources, and facilities provided by the National Computing Center of National Applied Research Laboratories of Taiwan under the funding support of the Ministry of Science and Technology of Taiwan, Contract Number MOST 110-2222-E-008-009-MY2. We also appreciate the efforts of Associate Researcher C.-M. Chang of Taiwan Instrument Research Institute of National Applied Research Laboratories of Taiwan and the helpful assistance of Y.-W. Chiang, Y.-S. Lin, C.-W. Yang, C.-C. Li, Y.-S. Liaw, and C.-H. Wang.

References

1 G. Dai, J. Min, H. Lu, H. Chang, Z. Sun, S. Ji, J. Lu, and L. Chang: J. Mater. Res. Technol. **24** (2023) 7021. https://doi.org/10.1016/j.jmrt.2023.04.261

2 C. Tan, R. Li, J. Su, D. Du, Y. Du, B. Attard, Y. Chew, H. Zhang, E. J. Lavernia, Y. Fautrelle, J. Teng, and A. Dong: Int. J. Mach. Tools Manuf. **189** (2023) 104032. https://doi.org/10.1016/j.msea.2023.145165

3 S. Afkhami, K. Lipiäinen, V. Javaheri, M. Amraei, A. Salminen, and T. Björk: Mater. Sci. Eng. A **876** (2023) 145165. https://doi.org/10.1016/j.msea.2023.145165

4 O. Pastushok, L. Kivijärvi, E. Laakso, M. Haukka, H. Piili, and E. Repo: Electrochim. Acta **440** (2023) 141732. https://doi.org/10.1016/j.electacta.2022.141732

5 A. Mussatto: Results Eng. **16** (2022) 100769. https://doi.org/10.1016/j.rineng.2022.100769

6 L.-F. Lai, D.-M. Lu, and J.-M. Lu: Sens. Mater. **34** (2022) 3911. https://doi.org/10.18494/SAM4030

7 L. Dejam, S. Kulesza, J. Sabbaghzadeh, A. Ghaderi, S. Solaymani, Ş. Ţălu, M. Bramowicz, M. Amouamouha, A. H. S. Shayegan, and A. H. Sari: Results Phys. **44** (2023) 106209. https://doi.org/10.1016/j.rinp.2023.106209

8 T. Zhu, X. Li, X. Zhao, X. Zhang, Y. Lu, and L. Zhang: Polym. Test. **106** (2022) 107460. https://doi.org/10.1016/j.polymertesting.2021.107460

9 A. A. Alghyamah, A. Y. Elnour, H. Shaikh, S. Haider, A. M. Poulose, S. M. Al-Zahrani, W. A. Almasry, and S. Y. Park: J. King Saud Univ-Com. **33** (2021) 101409. https://doi.org/10.1016/j.jksus.2021.101409

10 R. Mandal, S. Gangopadhyay, and A. Lahiri: Phys. Lett. B. **839** (2023) 137807. https://doi.org/10.1016/j.physletb.2023.137807

11 G. Clavier and A. P. Thompson: Comput. Phys. Commun. **286** (2023) 108674. https://doi.org/10.1016/j.cpc.2023.108674

12 T. Deguchi, T. Nakahara, and K. Imamura, and N. Ishida: Adv. Powder Technol. **32** (2021) 30. https://doi.org/10.1016/j.apt.2020.11.011

13 L. Chang, X. Liu, J. Zhao, and C. Zhou: J. Mater. Res. Technol. **17** (2022) 2118. https://doi.org/10.1016/j.jmrt.2022.01.122

14 M. Kulik and P. M. Dominiak: Comput. Struct. Biotechnol. J. **20** (2022) 6237. https://doi.org/10.1016/j.csbj.2022.10.018

15 M. S. Daw, S. M. Foiles, and M. I. Baskes: Mater. Sci. Rep. **9** (1993) 251. https://doi.org/10.1016/0920-2307(93)90001-U

16 W. Z. Polak: Comp. Mater. Sci. **201** (2022) 110882. https://doi.org/10.1016/j.commatsci.2021.110882

17 V. M. Gundyrev and V. I. Zel'dovich: Mat. Sci. Eng. A-struct. **481** (2008) 231. https://doi.org/10.1016/j.msea.2006.12.226

18 M. J. Saxton: Biophys. J. **110** (2016) 487a, https://doi.org/10.1016/j.bpj.2015.11.2604

19 L. Maragliano, G. Cottone, L. Cordone, and G. Ciccotti: Biophys. J. **86** (2004) 2765. https://doi.org/10.1016/S0006-3495(04)74330-1

About the Authors

Ling-Feng Lai received her B.S. and M.S. degrees from Chia Nan University of Pharmacy & Science (CNU), Taiwan, in 2015 and 2018, respectively. Since 2018, she has been a Ph.D. student at Southern Taiwan University of Science and Technology (NSUST), Taiwan. Her research interests include the molecular dynamics simulation of additive manufacturing. (da71y201@stust.edu.tw)

Yu-Chen Su received his Ph.D. degree from the University of Missouri, United States, in 2019. He is now an assistant professor in the Department of Civil Engineering at National Central University (NCU), Taiwan. Prior to joining NCU, Dr. Su worked as a postdoctoral researcher at the University of Mississippi. His research interests are in computational mechanics, molecular dynamics, and multiscale simulation for understanding mechanical behaviors for materials and solving engineering problems. (ycsu@ncu.edu.tw)

Deng-Maw Lu received his B.S. degree from Tamkang University, Taiwan, in 1979 and his M.S. and Ph.D. degrees from National Cheng Kung University (NCKU) in 1985 and 1996, respectively. From 1985 to 1988, he was a lecturer at NSUST, Taiwan. Since 1988, he has been a professor at NSUST. His research interests are in creative mechanism design, mechanical design, nanotechnology and simulation, and the history of science. (dmlu@stust.edu.tw)

Jian-Ming Lu received his Ph.D. degree from NCKU, Taiwan, in 2008. He has been a research fellow since 2015 and was an associate researcher at the National Center for High-Performance Computing (NCHC) of the National Applied Research Laboratories (NARL) in Taiwan from 2004 to 2015. His research interests are in nanomaterials, carbon nanotubes, molecular dynamics, and additive manufacturing. (0403817@narlabs.org.tw)

Kuei-Shu Hsu is a professor in the Department of Applied Geoinformatics of CNU. He received his M.S. degree in mechanical engineering and his Ph.D. degree from the Automation Control Group of Mechanical Engineering, Tatung University in 1997 and 2001, respectively. From 2001 to 2004, he was an assistant professor, and from 2005 to 2010, an associate professor in the Department of Applied Geoinformatics of CNU. In 2011, he became a professor. Currently, his research interests include the design, manufacture, and command of virtual reality systems, which include virtual reality and vehicle intelligent control via an integration system and a telerobotic system. (kshsu888@mail.cnu.edu.tw)